Improvement in Mechanical Properties of Poly(*p*-phenylene sulfide) Fibers by High-Tension Multiannealing Method

AKIHIRO SUZUKI, TAKAFUMI KOHNO

Department of Applied Chemistry and Biotechnology, Yamanashi University, 4-3-11 Takeda, Kofu 400-8511, Japan

Received 5 March 1999; accepted 25 June 1999

ABSTRACT: High-tension multiannealing (HTMA) was applied to improve the tensile properties of poly(*p*-phenylene sulfide) fibers, which was furthermore applied to the fibers produced and improved with the zone-drawing and zone-annealing treatments. The HTMA treatment was repeatedly applied to the fibers under the conditions of a 250°C temperature and an applied tension of between 201.0 and 188.0 MPa. As a result, at the 13th treatment the degree of crystallinity increased to 40%. On the other hand, the orientation factor of crystallites increased dramatically to 0.982 during the zone-drawing treatment, but increased only slightly during the subsequent treatments of zone annealing and HTMA. The finally obtained fiber had a tensile modulus of 10.4 GPa and a tensile strength of 0.73 GPa. © 2000 John Wiley & Sons, Inc. J Appl Polym Sci 75: 1569–1576, 2000

Key words: poly(*p*-phenylene sulfide) fiber; zone drawing and zone annealing; high-tension multiannealing; mechanical properties; viscoelastic properties

INTRODUCTION

Numerous studies[1–14] have undertaken the investigation of the crystalline structure, morphology, thermal stability, and crystallization kinetics of poly(*p*-phenylene sulfide) (PPS). However, only a limited number of articles have described the improvement in mechanical properties of PPS; Ito and Porter[15] reported a tensile modulus of 5.1 GPa and a tensile strength of 0.13 GPa using a solid coextrusion process. Carr and Ward[16] reported a tensile modulus of 8 GPa and a tensile strength of 0.7 GPa using a pin and plate process. We showed that the fiber produced by a zone-drawing (ZD) and zone-annealing (ZA) method had a tensile modulus of 8 GPa and a tensile strength of 0.7 GPa.[17]

To further improve the mechanical properties of fibers, it is necessary to more highly orient the amorphous chains because these chains play an important role in the determination of the mechanical properties in the drawing direction; however, it is difficult to improve the orientation of the amorphous chains in an oriented fiber. That is why the segmental mobility of the amorphous chains is severely constrained by the crystallites and molecular entanglements that act as physical crosslinks.[18]

In order to resolve the above problem and induce more crystallization, a high-tension annealing (HTA) method was carried out under an extremely high tension close to the tensile strength; this treatment was already applied to nylon 6, nylon 46, and nylon 66 fibers in our previous studies,[19–21] resulting in their respective mechanical properties being improved. In the present study we expected that a repeated HTA treatment might enable the further improvement of the mechanical properties. Therefore, an apparatus that automatically repeats the HTA treat-

Correspondence to: A. Suzuki.

Contract grant sponsor: Ministry of Education, Science, and Culture, Japan.

Journal of Applied Polymer Science, Vol. 75, 1569–1576 (2000)

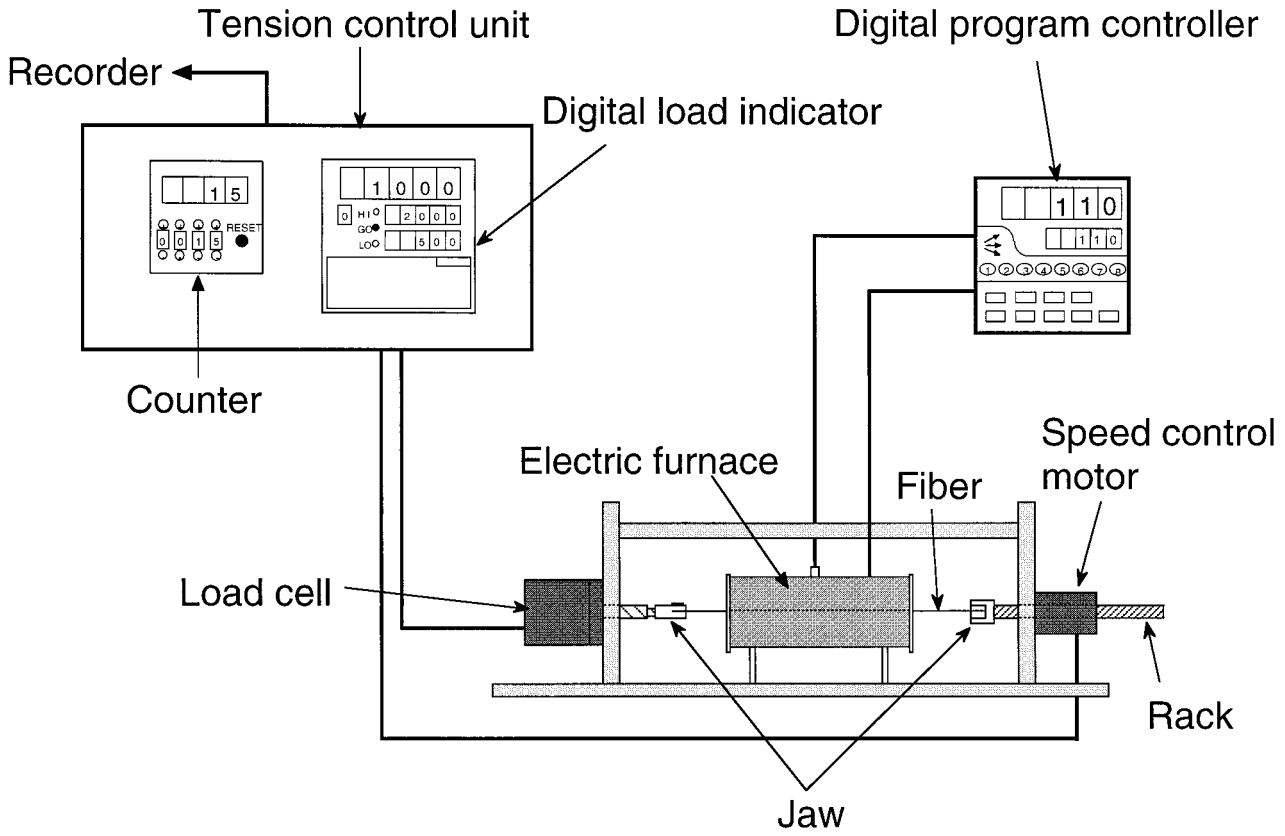

Figure 1 The apparatus used for the high-tension multiannealing (HTMA) method.

ment was assembled by modifying the conventional one for the HTA treatment. We refer to such a repeated HTA method treatment as a high-tension multiannealing (HTMA) treatment. In our previous study the HTMA treatment using the modified apparatus was applied to nylon 46 fiber, and we reported on the improvement of its mechanical properties.[22]

The objective of the present study was to further improve the mechanical properties of PPS fibers by applying the HTMA treatment. The effect of the HTMA treatment on the mechanical properties and superstructure was investigated by tensile testing, dynamic viscoelastometry, thermal mechanical analysis, X-ray diffraction, and density measurements.

EXPERIMENTAL

Materials

The original material was an as-spun PPS fiber supplied by Toray Ltd., which is the same as that for previous work.[17] The isotropic as-spun fiber had a diameter of about 0.4 mm and degree of crystallinity of 11%.

HTMA Treatments

A schematic diagram of the apparatus used for the HTMA treatment is given in Figure 1. It consists of a load cell, a 20 mm long electric furnace controlled by a digital program controller, a tension control unit, and a speed control motor with a linear head that converts the rotational motion of the motor into linear motion. The tension control unit is capable of setting the maximum and minimum applied tensions along with the number of repetitions. One end of the fiber is fixed at a jaw equipped with the load cell, and the other is run through the electric furnace and fixed at a jaw equipped with the edge of the rack. Figure 2 shows the change of applied tension (σ) during the HTMA treatment over time. When the temperature of the electric furnace reached a desired treating temperature (T_t), the fiber was stretched at a speed of 10 mm/min. When the σ value reached the set maximum applied tension (σ_{max}) the stretching stopped, and then the fiber was

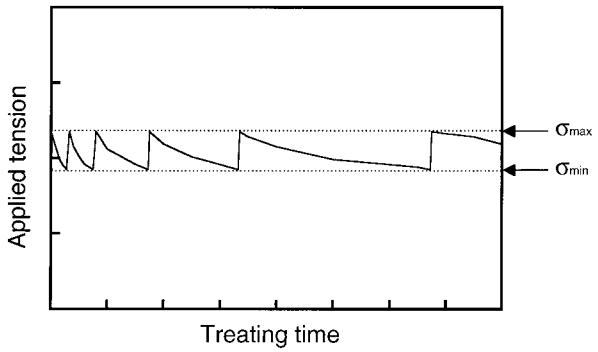

Figure 2 The scheme of the change in applied tension with treating time during the HTMA treatment.

kept under a constant length until the σ value decreased to the set minimum applied tension ($\sigma_{\min}$). When the σ value reached the $\sigma_{\min}$ value the fiber was automatically stretched at 10 mm/min until the σ value increased to the $\sigma_{\max}$ value again. The HTMA treatment was carried out up to the predetermined number of repetitions. The $\sigma_{\max}$ value was determined within the range of 70–90% of the strength at the break (σ_b), which was previously estimated from the stress–strain curve recorded at the same temperature as T_t. The $\sigma_{\min}$ value was determined on the basis of a pseudoequilibrium value given in the σ versus T_t curve. The reduction in the σ was not attributed to the orientational relaxation due to a slippage among molecular chains, but to the improvement of amorphous chain orientation and to the spontaneous elongation due to an additional crystallization. This is supported by the fact that the amorphous orientation and crystallinity of the fibers[19–22] developed during the HTA treatments. The treating time required for each step increased exponentially with the number of repetitions of the HTMA treatments.

Measurement

The draw ratio was determined in the usual way by measuring the displacement of ink marks placed 10 mm apart on the fiber before drawing.

The density (ρ) of the fiber was measured at 23°C by a flotation technique using a carbon tetrachloride and toluene mixture. The degree of crystallinity, expressed as a weight fraction (X_w), was obtained using the relation

$$X_w = \{\rho_c(\rho - \rho_a)\}/\{\rho(\rho_c - \rho_a)\} \times 100 \qquad (1)$$

where ρ_c and ρ_a are the densities of the crystalline and amorphous phases, respectively. In this measurement a value of 1.43 g/mL was assumed for ρ_c,[23] and a value of 1.31 g/mL was assumed for ρ_a.[23] The density of the amorphous polymer was assumed to be constant and independent of treatments.

Thermal shrinkage was measured with a Rigaku SS-TMA at a heating rate of 5°C/min. The samples with a 15-mm gauge length between the two jaws were held under a tension of 5 g/cm^2, which was the minimum value to stretch the fibers tightly.

The orientation factors of the crystallites (f_c) were evaluated using the Wilchinsky[24] method from wide angle X-ray diffraction patterns. The f_c values were estimated by using the (200) plane.

The apparent crystallite sizes were estimated from the broadening of the diffraction peaks by applying Scherrer's equation

$$D_{\text{hkl}} = 0.9\lambda/\beta \cos \theta_{\text{hkl}} \qquad (2)$$

where D_{hkl} is the crystallite width normal to the (hkl) plane; λ is the X-ray wavelength (1.542 Å); θ_{hkl} is the Bragg angle of the (hkl) plane; and β is the observed half-width of the peaks, which was calibrated for an instrumental broadening.

The tensile modulus, tensile strength, and elongation at break were measured at 23°C using a Tensilon tensile testing machine with a sample length of 50 mm and a rate of 10 mm/min.

The dynamic viscoelastic properties were measured at 110 Hz with a dynamic viscoelastometer (Vibron DDV-II, Orientec Co. Ltd.). Measurements were carried out over a temperature range of 25 to about 260°C at intervals of 5°C, and the average heating rate was 2°C/min. The fiber was held in a 20-mm gauge length between the two jaws.

RESULTS AND DISCUSSION

Optimum Conditions of HTMA

The original PPS fiber was initially treated with the ZD and ZA treatments before the HTMA treatment. The ZD and ZA treatments were carried out under the same optimum conditions as those determined in our previous work,[17] and the conditions of the ZD and ZA treatments are given in Table I. The ZA fiber obtained had a degree of crystallinity of 38%, a tensile modulus of 8.0 GPa, and a tensile strength of 0.68 GPa.

Table I Optimum Conditions for Zone-Drawing (ZD) and -Annealing (ZA) Treatments

Treatment	Treating Temp. (°C)	Applied Tension (MPa)
ZD	90	5.5
ZA	220	138.0

The HTMA treatments under various conditions were carried out to obtain the optimum temperature (T_t), σ_{max}, and σ_{min} values and the number of repetitions (n_t) of the HTMA treatment. As a result the optimum condition was determined by measuring the dynamic viscoelastic properties.

Figure 3 shows the changes in the storage modulus (E') at 25°C for the fibers treated under three different σ_{max} values with the T_t. The σ_{max} values were 70, 80, and 90% of the strength at break (σ_b). The σ_b value was estimated from the stress–strain curve measured at each T_t. The E' values of the fiber treated at each σ_{max} increase with T_t, but the fiber treated under $0.9\sigma_b$ at T_t = 250°C was broken during the HTMA treatment. Consequently, the fibers treated under $0.7\sigma_b$ and $0.8\sigma_b$ at T_t = 250°C had the maximum E' values, and the fibers drawn under $0.7\sigma_b$ at T_t = 250°C had almost the same value as that of the fiber treated under $0.9\sigma_b$ at T_t = 220°C. In addition, the effect of n_t on the mechanical properties was studied on the fibers treated under $0.7\sigma_b$ and $0.8\sigma_b$ at T_t = 250°C. The optimum σ_{min} value for each condition was found through our preliminary experiments to be at $0.65\sigma_b$.

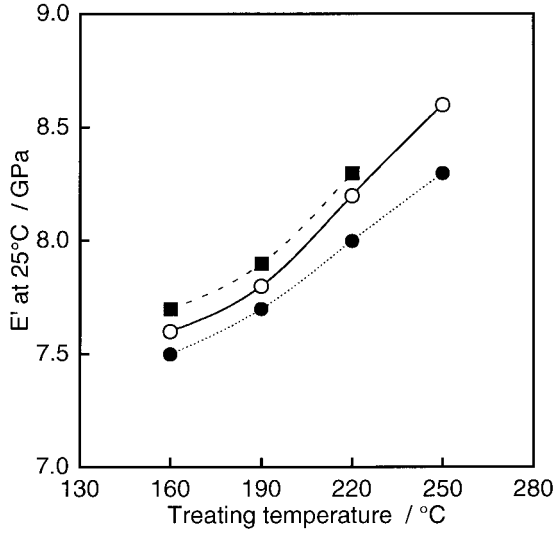

Figure 3 The changes in the storage modulus (E') at 25°C for the fibers obtained at three different maximum applied tensions (σ_{max}) with treating temperature: σ_{max} = (■) $0.9\sigma_b$, (○) $0.8\sigma_b$, and (●) $0.7\sigma_b$.

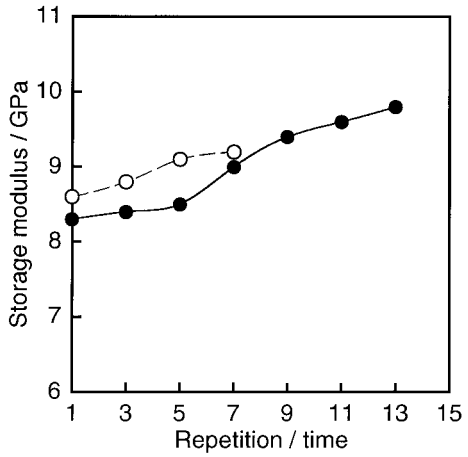

Figure 4 The changes in the storage modulus (E') at 25°C with the number of repetitions (n_t) for the fibers treated at 250°C under σ_{max} = (●) $0.7\sigma_b$ and (○) $0.8\sigma_b$.

Figure 4 shows the changes of the E' at 25°C with n_t. The E' value of the fiber treated under $\sigma_{max} = 0.7\sigma_b$ increased with n_t up to the 13th treatment, above which value the change in E' with n_t was small. However, the fiber treated under $0.8\sigma_b$ broke during the 8th treatment, and then the treatment under $0.8\sigma_b$ was only carried out up to n_t = 7. Table II shows the optimum condition for the HTMA treatment.

Microstructure for ZD, ZA, and HTMA Fibers

Table III shows the draw ratio (λ), degree of crystallinity (X_w), crystallite orientation factor (f_c), and apparent crystallite sizes normal to the (110) and (200) planes (D_{110}, D_{200}) for the original, ZD, ZA, and HTMA fibers. The X_w value increased from 11% for the original fiber to 40% for the HTMA fiber. The X_w values achieved were lower than that (X_w = 55%) of the poly(ethylene terephthalate) (PET) fibers.[25] It is difficult to crystallize the PPS fiber compared to the PET fiber because the high electron density of the sulfur and phenylene groups restricts the free rotation of the C—S bond.[16]

The crystallite sizes (D_{110}, D_{200}) increased stepwise with processing. The corresponding values of the HTMA fiber were almost 1.5 and 2 times higher than those obtained from the ZD fibers, respectively. The HTMA nylon 46 fiber[22]

Table II Optimum Conditions for HTMA Treatment

Treatment	Treating Temp. (°C)	Applied Tension (MPa)	Repetitions
HTMA	250	σ_{max} = 201 (0.7σ_b) σ_{min} = 188 (0.65σ_b)	13

σ_b = 287.1 MPa at 250°C.

crystallite sizes (D_{100}, D_{010}) were held constant throughout the whole treatment, although the X_w value increased with processing. Therefore, we considered that the increase in X_w showed the evolution of crystallization along the drawing direction. It is well known that an additional crystallization in an oriented material is much faster than that in its isotropic one[26–28] and that the crystallization occurs along the fiber axis of the already oriented crystals.[29] However, the results from the PPS fiber seem to indicate that the crystallization is not only perpendicular but also parallel to the drawing direction.

The f_c value was increased dramatically up to 0.982 by the ZD treatment and slightly during the subsequent treatments. Murthy et al.[30] reported that the crystalline orientation increased rapidly at small draw ratios (<3) and reached a plateau at higher draw ratios.

Figure 5 shows the temperature dependence of thermal shrinkage for the original, ZD, ZA, and HTMA fibers. The development of the thermal shrinkage during heating is associated with chain coiling in the oriented amorphous regions.[31] The shrinkage depends on both the amorphous orientation and the crosslink density of the physical network formed from crystallites. The original fiber elongated rapidly above 90°C and the elongation exceeded our instrument capability. The elongation behavior of the original fiber is much different from that of the original PET fiber.[25] The PET fiber elongated rapidly in the temperature range of 70–100°C and slowly above 100°C without exhibiting fluidlike deformation. The behavior of the PET fiber suggested that the crystallites were formed by the strain-induced crystallization developed in the temperature range during the measurement and that the additional slippage of the chains was constrained by the physical network made up of crystallites. However, the rapid elongation of the original PPS fiber showed that no network preventing fluidlike deformation existed and that no strain-induced crystallization occurred during the measurement.

On the other hand, the ZD, ZA, and HTMA fibers shrank with the temperature above the glass transition (T_g); however, the ZD fiber behavior was different than those of ZA and HTMA fibers. The ZD fiber shrank rapidly in the temperature range of 100–120°C, slowly in the temperature range of 120–250°C, and then rapidly again above 250°C. The ZA and HTMA fibers shrank slowly above 70°C, but a small difference was seen between the ZA and HTMA fibers at the high temperature. The differences in the behavior of the shrinkage regarding the ZD, ZA, and HTMA fibers may be due to the respective crosslink densities of the physical network. The physical network of the ZD fiber was insufficient for the constraint of the thermal shrinkage because of its low X_w as compared to the ZA and HTMA fibers. The shrinkage decreased above 120°C because of an increase in the crosslink density resulting from additional crystallization of the amorphous

Table III Draw Ratio (λ), Degree of Crystallinity (X_w), Crystallite Orientation Factor (f_c), and Crystallite Size (D_{110}, D_{200}) Planes for Fibers

Treatment	λ	X_w (%)	f_c	D_{110} (Å)	D_{200} (Å)
Original	—	11	—	—	—
ZD	4.3	16	0.982	31	22
ZA	6.0	38	0.986	37	35.1
HTMA	6.6	40	0.988	47	42.5

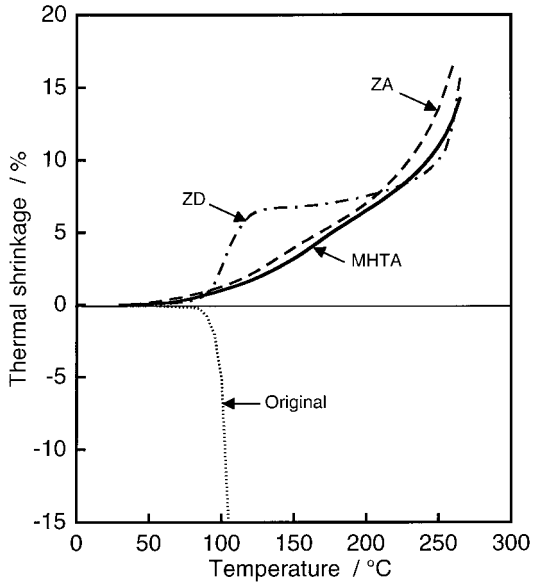

Figure 5 The temperature dependence of the shrinkage for the original, ZD, ZA, and HTMA fibers.

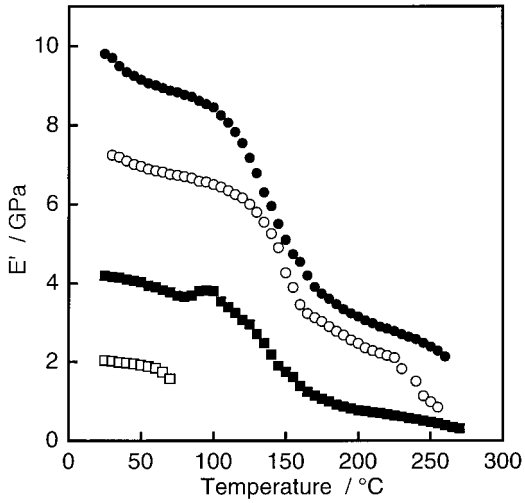

Figure 6 The storage modulus (E') as a function of temperature at 110 Hz for the original, ZD, ZA, and HTMA fibers: (□) original, (■) ZD, (○) ZA, and (●) HTMA.

chains oriented during measurement.[29] When the ZA and HTMA fibers had a higher X_w value, the oriented amorphous chains were constrained by the physical network, which had a higher crosslink density, and the chain became increasingly difficult to coil. The TMA curves of the ZA and HTMA fibers showed that only a small difference in X_w affects the shrinkage behavior. The significant increase observed above 250°C resulted from an increase in segmental motion at a higher temperature and a decrease in the crosslink density of the network attributed to the partial melting of the crystallites with lower perfection.

Mechanical Properties for ZD, ZA, and HTMA Fibers

The tensile properties of the original ZD, ZA, and HTMA fibers are given in Table IV. The HTMA fiber has a tensile modulus of 10.4 GPa and a tensile strength of 0.73 GPa. The values are higher than those of the commercial PPS fibers (3–7 and 0.53–0.65 GPa). The tensile modulus of the ZA fiber corresponds to 26% of a theoretical value[16] (40 GPa at room temperature).

Table IV Tensile Properties for Fibers

Fiber	Tensile Modulus (GPa)	Tensile Strength (GPa)	Elongation at Break (%)
Original	2.7	11	491.9
ZD	5.2	16	24.5
ZA	8.0	38	11.4
HTMA	10.4	40	8.8

Figure 6 shows the temperature dependence of the storage modulus (E') for the original, ZD, ZA, and HTMA fibers. The viscoelastic properties for the original fiber could not be measured above T_g because of the fluidlike deformation. The flow deformation is caused by a slippage among the amorphous chains because the physical network is absent from the original fiber as described above. The E' values of the ZD fiber decrease with increasing temperature and increase slightly in the temperature range of 90–100°C, and then the E' values start to decrease again. Such a slight increment of the E' is attributable to an additional increase in the crosslink density of the network resulting from strain-induced crystallization developed during the measurement. For the HTMA fiber the E' value reaches 9.8 GPa at 25°C and decreases with increasing temperature, and a significant decrease resulting from the glass transition is observed in the temperature range of 110–160°C.

Figure 7 shows the temperature dependence of the tan δ for the original, ZD, ZA, and HTMA fibers. The treated fibers show α relaxations at about 150°C, which are considered to originate from the glass transition.[32] Lukashov et al.[33] re-

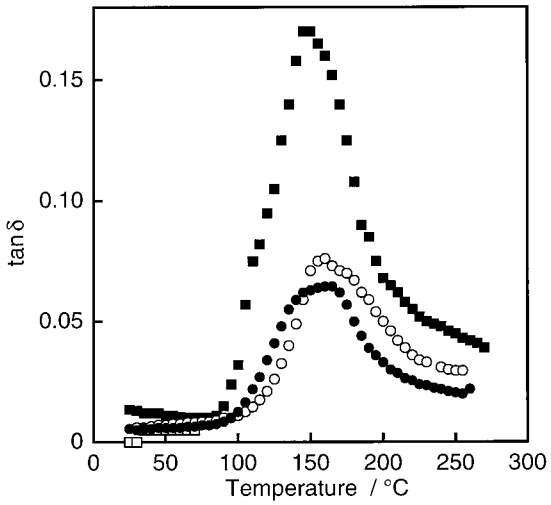

Figure 7 The tan δ as a function of temperature at 110 Hz for the original, ZD, ZA, and HTMA fibers: (□) original, (■) ZD, (○) ZA, and (●) HTMA.

ported that the relaxation related to the unfreezing of the cooperative segmental motion in a random polymer matrix was observed at about 60°C. However, no relaxation peak at 60°C was observed in the tan δ versus temperature curve. The ZD fiber has an α-relaxation peak at 145°C, and the trace of a shoulder is caused at 110°C by the strain-induced crystallization developed during the measurement. The α peak shifts to the higher temperature, and its value decreases markedly in peak height with the processing. The HTMA fiber shows a broad α-relaxation peak at 165°C, and its magnitude is about one-third of that of the ZD fiber. The changes in the position and profile of the α peak with processing indicate that the molecular mobility in the amorphous regions is restricted by the physical network with a higher degree of crosslink density.

CONCLUSION

Our experimental data discussed here show that the HTMA treatment is effective in improving the mechanical properties of PPS fibers. The results are as follows:

1. The degree of crystallinity increased to 38% with the ZD and ZA treatments and increased to 40% with the HTMA treatment. The orientation factor of crystallites increased remarkably up to 0.982 with only the ZD treatment and increased slightly during the subsequent treatments. This fact indicates that the orientational relaxation of crystallites due to a slippage among molecular chains did not occur during the HTMA treatment.
2. The HTMA fiber showed a tensile modulus of 10.4 GPa and a tensile strength of 0.73 GPa. The α peak in the temperature dependence of tan δ shifted to a higher temperature and progressively reduced its magnitude in the process of treatment. The changes in the position and profile of the α peak pointed out that the molecular mobility in the amorphous regions was restricted by their surrounding crystallites.

We are grateful to Toray Ltd. for supplying the PPS fibers to us.

REFERENCES

1. Lovinger, A. J.; Padden, F. J., Jr.; Davis, D. D. Polymer 1998, 29, 229.
2. Brauman, S. K. J Polym Sci Polym Chem Ed 1989, 27, 3285.
3. Woo, E. M.; Chen, J. M. J Polym Sci Phys Chem Ed 1995, 33, 1985.
4. Risch, B. G.; Srinicvas, S.; Wilkes, G. L.; Geibel, J. F.; Ash, C.; White, S.; Hicks, M. Polymer 1996, 37, 3623.
5. Clarke, T. C.; Kanazawa, K. K.; Lee, V. Y.; Rabolt, J. F.; Reynolds, J. R.; Street, G. B. J Polym Sci Polym Phys Ed 1982, 20, 117.
6. Elsenbaumer, R. L.; Shacklette, L. W. J Polym Sci Polym Phys Ed 1982, 20, 1781.
7. Radhakrishnan, S.; Joshi, S. G. J Polym Sci Polym Phys Ed 1989, 27, 127.
8. Hruszka, P.; Jurga, J.; Kubis, J.; Pislewski, N. Polymer 1991, 32, 1589.
9. Campos, M.; Cavalcante, E. M.; Kalinowski, J. J Polym Sci Polym Phys Ed 1996, 34, 623.
10. Zhang, X.; Wang, Y. Polymer 1989, 30, 1867.
11. Subramanian, P. R.; Isayev, A. I. Polymer 1991, 32, 1961.
12. Minkova, L. I.; Magagnini, P. I. Polymer 1995, 36, 2059.
13. Gopakumar, T. G.; Ghadage, R. S.; Ponrathnam, S.; Rajan, C. R.; Fradet, A. Polymer 1997, 38, 2209.
14. Choi, J.; Lim, S.; Kim, J.; Choe, C. Polymer 1997, 38, 4401.
15. Ito, M.; Porter, R. S. J Polym Sci Polym Phys Ed 1985, 23, 245.
16. Carr, P. L.; Ward, I. M. Polymer 1987, 28, 2070.
17. Suzuki, A.; Kohno, T.; Kunugi, T. J Polym Sci Polym Phys Ed 1998, 36, 1731.

18. Chuah, H. H.; Porter, R. S. Polymer 1986, 27, 241.
19. Suzuki, A.; Kondo, M.; Kunugi, T. Kobunshi Ronbunsyu 1993, 50, 93.
20. Suzuki, A.; Endo, A.; Kunugi, T. Polym J 1998, 30, 275.
21. Suzuki, A.; Murata, H.; Kunugi, T. Polymer 1998, 39, 1351.
22. Suzuki, A.; Endo, A.; Kunugi, T. J Polym Sci Polym Phys Ed 1998, 36, 2737.
23. Tabor, B. J.; Magre, E. P.; Boon, J. Eur Polym J 1971, 7, 1127.
24. Wilchinsky, Z. W. J Appl Phys 1963, 30, 792.
25. Suzuki, A.; Sato, Y.; Kunugi, T. J Polym Sci Polym Phys Ed 1998, 36, 473.
26. Smith, F. S.; Steward, R. D. Polymer 1974, 15, 283.
27. Alfonso, G. C.; Verdona, M. P.; Wasiak, A. Polymer 1978, 19, 711.
28. Gupte, K. M.; Motz, H.; Schultz, J. M. J Polym Sci Polym Phys Ed 1983, 21, 1927.
29. Peszkin, N. P.; Schultz, J. M.; Lin, J. S. J Polym Sci 1986, 24, 2591.
30. Murthy, N. S.; Bray, R. G.; Correale, S. T.; Moore, R. A. F. Polymer 1995, 36, 3863.
31. Wilson, M. P. W. Polymer 1974, 15, 277.
32. Rigby, S. J.; Dew-Hughes, D. Polymer 1974, 15, 639.
33. Lukashov, A.; Feofanov, V.; Schultze, J. D.; Boehning, M.; Springer, J. Polymer 1992, 33, 2227.